

# Reduction of Radar Cross Section Based on a Metasurface

Jie Chen, Qiang Cheng<sup>\*</sup>, Jie Zhao, Di Sha Dong, and Tie Jun Cui

**Abstract**—A metasurface for Radar Cross Section (RCS) reduction is proposed. The surface is composed of the same type of metamaterial units with different geometric dimensions, leading to various reflection phases under the incidence of plane waves. By carefully choosing the phase distributions, diffusion will be produced for the reflected waves which may redistribute the scattering energy from the surface toward all the directions, and hence it can be applied as the coating of metallic targets with ultra-low RCS. Both the simulated and experimental results have validated the proposed method.

## 1. INTRODUCTION

In recent years, metamaterials exhibiting unusual permittivity and permeability have received much attention due to their exotic electromagnetic (EM) properties that natural materials do not have [1–6]. Metamaterials are usually composed of periodic resonant or non-resonant structures, and can be regarded as electromagnetic materials when the dimension of the unit cell is much smaller than the wavelength in free space according to effective medium theory [7]. To date, a number of interesting applications have been proposed and experimentally verified, such as the gradient index lens, invisible cloak and sub-wavelength imaging [8–16].

In addition, the potential application of metamaterials in stealth technology also becomes a hot topic of current research [17–20], where RCS [21–24] is the main consideration in the design of military platforms. There are two different solutions proposed for RCS reduction using metamaterials: cloaking devices [25] and metamaterial absorber. The cloaking devices are actually metamaterial shells which can guide EM fields around the internal objects without perturbing the exterior fields. Some interesting cloaking devices have been experimentally verified, such as the free-space cloak by Schurig et al. and the carpet cloak by Liu et al. [9, 10]. The metamaterial absorber utilizes the loss components of the effective medium parameters to absorb the energy of incident waves, which is much thinner than traditional absorbing materials [26–30].

In this paper, a metasurface is designed and tested for backward RCS reduction. Different from the two techniques mentioned above, the metasurface can cause diffusion of reflected waves [31–33] and hence redistribute the scattering energy from the objects under the metasurface into the whole space, leading to significantly reduced RCS verified by the simulation and experimental results later.

## 2. THEORETICAL ANALYSIS AND NUMERICAL ANALYSIS

The principle of the proposed metasurface is quite simple: The metasurface is composed of a number of unit cells with various resonant frequencies, and each unit has different reflection phase for the same incident wave. When the phase distributions at the surface tend to be randomly distributed, diffusion will be produced for waves reflected at the surface. Hence the reflected energy in the direction of incoming waves will be greatly reduced.

---

*Received 26 February 2014, Accepted 11 April 2014, Scheduled 29 April 2014*

<sup>\*</sup> Corresponding author: Qiang Cheng (qiangcheng@seu.edu.cn).

The authors are with the State Key Laboratory of Millimeter Waves, Department of Radio Engineering, Southeast University, Nanjing 210096, China.

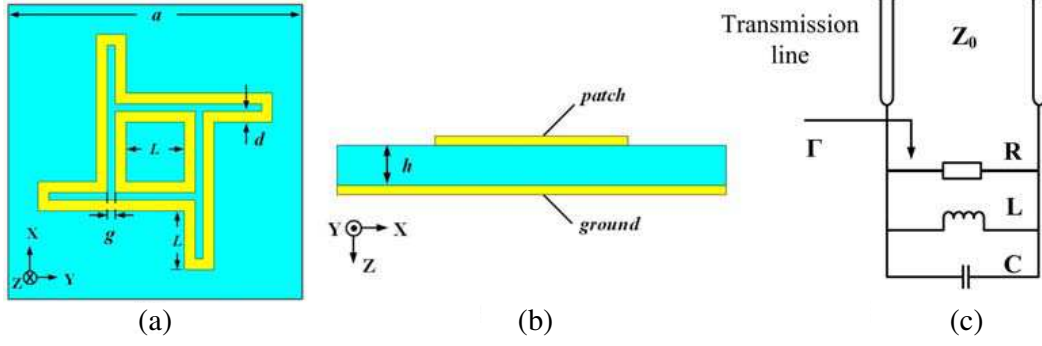


**Figure 1.** (a) The front view and (b) the lateral view of the basic unit, where  $a = 15$  mm,  $h = 4$  mm,  $g = 0.4$  mm,  $d = 0.55$  m. (c) Effective circuit model of the basic unit.

The basic phasing element of the metasurface is shown in Fig. 1, which is a windmill-shaped patch on the substrate F4B ( $\epsilon_r = 2.65$ ). The element was firstly proposed in the design of broadband reflectarray antenna [34]. Compared to the traditional single-layer structures, the windmill-shaped element has the advantage of larger phase variation and broad bandwidth. We assume that the metasurface is coated upon a metallic plate, so in the simulation we add a ground layer under the substrate (see Fig. 1(b)). The interaction between EM waves and the phasing element can be understood from the effective circuit model as illustrated in Fig. 1(c), and the reflection phase of the unit could be written as (1)

$$\varphi = \tan^{-1} \left( \frac{X}{R - Z_0} \right) - \tan^{-1} \left( \frac{X}{R + Z_0} \right) \quad (1)$$

$$X = - \left( \omega C - \frac{1}{\omega L} \right) / \left[ \left( \omega C - \frac{1}{\omega L} \right)^2 + \frac{1}{R^2} \right] \quad (2)$$

and the phase rate of change can be expressed as (3).

$$\xi_0 = \frac{4RZ_0Q}{\omega_0(R^2 - Z_0^2)} \quad (3)$$

where  $Z_0$  is the wave impedance of free space, and  $R$ ,  $L$ ,  $C$  are the equivalent resistance, inductance and capacitance of the windmill-shaped patch in Fig. 1, respectively.  $Q$  is the quality factor,  $X$  the equivalent reactance, and  $\omega_0$  the resonant frequency of the basic unit. In order to obtain a broadband phasing element, the phase rate of change shall be as flat as possible near the resonant frequency, which requires low quality factor as indicated in Eq. (3). Due to the low permittivity of the substrate, we need to increase the substrate thickness to further lower the quality factor and improve the phase linearity. An inner square ring has been inserted into windmill-shaped unit to avoid the decrease of the total phase range by introducing another resonant frequency [34]. To validate the broadband property of the windmill-shaped unit, we have plotted the corresponding reflection phase within X band, as illustrated in Fig. 2(a), where  $a = 15$  mm,  $h = 4$  mm,  $g = 0.4$  mm,  $d = 0.55$  mm. It is obvious that the unit has nearly linear frequency response when the ring length  $L$  changes from 0.8 mm to 3.2 mm. From Fig. 2(b), the reflection phase varies linearly with the change of  $L$  at  $f = 10$  GHz, ranging from  $0^\circ$  to  $360^\circ$  as required.

Next we will discuss the design of the whole metasurface, which is composed of  $20 \times 20$  units as shown in Fig. 3. In order to disperse the reflection energy into the whole space, we consider the random phase distribution on the metasurface. Four hundred stochastic numbers are generated firstly between 0 and 360. From the relation between the unit dimension  $L$  and the reflection phase, we can easily get the desired metasurface pattern. Full wave simulations have been made to compute the far field RCS of the designed metasurface using the commercial software CST 2011. The RCS distributions of a bare metallic plate and a metallic plate coated with the metasurface have been plotted in Figs. 4(a)–4(e), where the operation frequency is chosen to be 8, 9, 10, 11 and 12 GHz respectively. When the metallic plate is covered by the metasurface, a significant RCS reduction has been obtained in the normal direction, which is more than 10 dB within the whole X band as shown in Fig. 6. The maximum RCS reduction

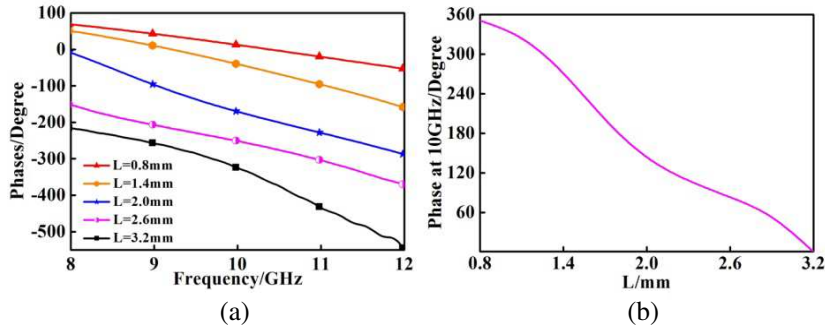


**Figure 2.** Phase distribution of the reflected electric field with (a) different L within X band and (b) at 10 GHz.

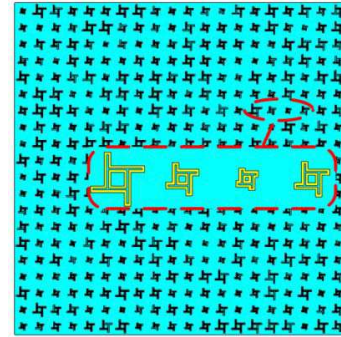


**Figure 3.** The metasurface for RCS reduction in the simulation.

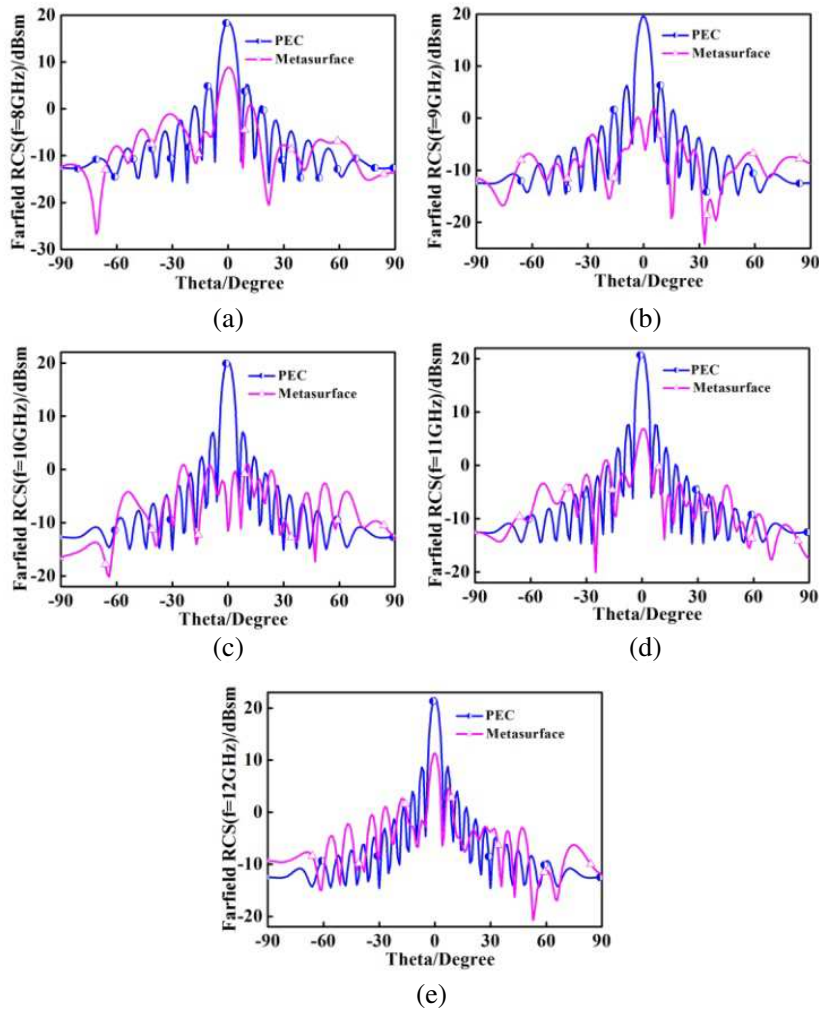


**Figure 4.** Simulated far-field scattering pattern for naked PEC plate and the metasurface under normal incidence at (a) 8 GHz, (b) 9 GHz, (c) 10 GHz, (d) 11 GHz, (e) 12 GHz.

can be achieved near the center frequency  $f = 10$  GHz, which is nearly 25 dB. In some other directions, the RCS is increased a little due to the random scattering at the metasurface. However, since they do not appear in the main scattering directions, it will not increase the detection probability of the metallic objects obviously.

### 3. FABRICATION AND EXPERIMENT

In order to verify the theoretical analysis stated above, a metasurface has been fabricated and tested, as shown in Fig. 5(a). The dielectric substrate F4B, with the permittivity 2.65 and the loss tangent 0.001 has been used, where the substrate thickness is  $h = 4$  mm. The back of sample is covered by a copper layer with the metallization thickness 0.035 mm. To guarantee the accuracy of measurement, the sample are usually chosen to be square in shape, whose dimension is larger than  $5\lambda$  and less than  $15\lambda$  ( $\lambda$  is the operating wavelength). To meet that requirement, we place altogether  $20 * 20$  unit cells in the whole sample, and the periodicity of each unit is 15 mm. The experimental setup has been illustrated in Fig. 5(b), where the transmitting and receiving horn antennas in the X band have been connected to a vector network analyzer (Agilent N5230C) to measure the far field radiation pattern of the designed metasurface. In this experiment, the height of the sample is kept the same as that of the antennas. Also the antennas are placed far enough from the sample ( $> 2D^2/\lambda$ ) to avoid the near field effect. Pyramid absorbing materials have been placed around the sample to decrease the unwanted reflections from the surroundings. What's more, we can rotate the sample to evaluate the scattering properties for waves incident obliquely with the angle ranging from  $0^\circ$  to  $20^\circ$ .

Here we consider the monostatic RCS reduction, where we have measured the reflection coefficient from a bare metallic plate and the metasurface sample. The transmitting and receiving antennas are placed closely. After some mathematical manipulating, we can get the difference of the RCS in the two cases (as shown in Fig. 6(a) and Fig. 6(b)) for the  $x$  and  $y$  polarization, from which we can see that the metasurface can effectively decrease the scattering from the bare metallic plate. It is clear that the RCS can be reduced by more than 10 dB from 8 GHz to 13 GHz. The maximum of the RCS reduction curve could be found at  $f = 12$  GHz for  $TE$  polarization, which is nearly 30 dB as we can see in Fig. 6(a). There is a frequency shift between the simulation and experimental results, which is possibly due to the

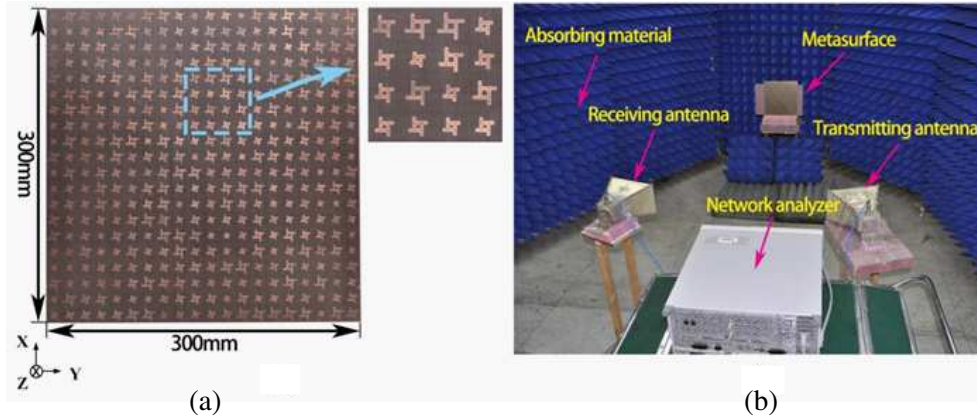


**Figure 5.** (a) The fabricated metasurface and (b) the experimental setup.

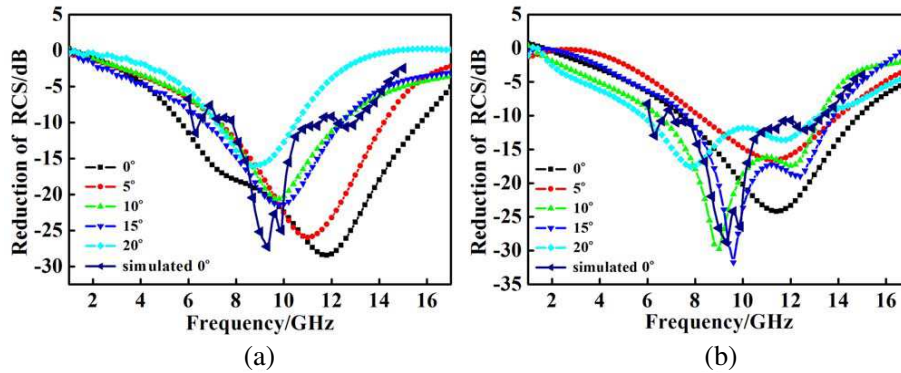


**Figure 6.** Simulated and measured monostatic RCS reduction for various incident angles for (a)  $x$  polarization and (b)  $y$  polarization.

fabrication error and the variation of the dielectric constant with respect to the standard value presented by the manufacturer [19]. Next we rotate the sample to measure the backward RCS of the metallic plate and the metasurface sample under oblique incidence. Four typical incident angles ( $5^\circ$ ,  $10^\circ$ ,  $15^\circ$ ,  $20^\circ$ ) have been selected in the experiment. From Fig. 6, we can see that the reduction approaches to a lower level with the increase of the incident angle, since the reflection from the metallic plate decrease dramatically under oblique incidence. However, it still keeps higher than 10 dB within the whole X band, showing excellent broadband properties as expected.

#### 4. CONCLUSIONS

In conclusion, a broadband metasurface for backward RCS reduction has been designed and tested. By controlling the phase distributions on the metasurface, diffusion can be caused for the reflected waves, leading to significant backward RCS reduction. The measured results show that the metasurface can effectively decrease the backward scattering within the whole X band under normal and oblique incidences when coating on a metallic plate, which may find potential applications in the stealth technology in the future.

#### ACKNOWLEDGMENT

This work was supported by the National Natural Science Foundation of China (60990320, 60901011 and 60990324), National High Tech (863) Projects (2011AA010202 and 2012AA030402), 111 Project (111-2-05) and the Natural Science Foundation of the Jiangsu Province BK2010394 and BK2012019, and 20130202 Guangxi Experiment Center of Information Science, Guilin University of Electronic Technology.

#### REFERENCES

1. Pendry, J., A. Holden, W. Stewart, and I. Youngs, "Extremely low frequency plasmons in metallic mesostructures," *Physical Review Letters*, Vol. 76, No. 25, 4773, 1996.
2. Pendry, J., A. Holden, D. Robbins, and W. Stewart, "Magnetism from conductors and enhanced nonlinear phenomena," *IEEE Transactions on Microwave Theory and Techniques*, Vol. 47, No. 11, 2075, 1999.
3. Shelby, R. A., D. R. Smith, and S. Schultz, "Experimental verification of a negative index of refraction," *Science*, Vol. 292, No. 5514, 77–79, 2001.
4. Smith, D., J. Pendry, and M. Wiltshire, "Metamaterials and negative refractive index," *Science*, Vol. 305, No. 5685, 788–792, 2004.
5. Pendry, J., "A chiral route to negative refraction," *Science*, Vol. 306, No. 5700, 1353–1355, 2004.
6. Soukoulis, C. M., "Physics: Negative refractive index at optical," *Science*, Vol. 1136481, No. 47, 315, 2007.
7. Smith, D., S. Schultz, P. Markoš, and C. Soukoulis, "Determination of effective permittivity and permeability of metamaterials from reflection and transmission coefficients," *Physical Review B*, Vol. 65, No. 19, 195104, 2002.
8. Ma, H. F., X. Chen, H. S. Xu, X. M. Yang, W. X. Jiang, and T. J. Cui, "Experiments on high-performance beam-scanning antennas made of gradient-index metamaterials," *Applied Physics Letters*, Vol. 95, No. 9, 094107–094107-3, 2009.
9. Schurig, D., J. Mock, B. Justice, S. Cummer, J. Pendry, A. Starr, and D. Smith, "Metamaterial electromagnetic cloak at microwave frequencies," *Science*, Vol. 314, No. 5801, 977–980, 2006.
10. Liu, R., C. Ji, J. Mock, J. Chin, T. Cui, and D. Smith, "Broadband ground-plane cloak," *Science*, Vol. 323, No. 5912, 366–369, 2009.
11. Valentine, J., J. Li, T. Zentgraf, G. Bartal, and X. Zhang, "An optical cloak made of dielectrics," *Nature Materials*, Vol. 8, No. 7, 568–571, 2009.
12. Ergin, T., N. Stenger, P. Brenner, J. B. Pendry, and M. Wegener, "Three-dimensional invisibility cloak at optical wavelengths," *Science*, Vol. 328, No. 5976, 337–339, 2010.
13. Gömöry, F., M. Solov'yov, J. Šouc, C. Navau, J. Prat-Camps, and A. Sanchez, "Experimental realization of a magnetic cloak," *Science*, Vol. 335, No. 6075, 1466–1468, 2012.

14. Wood, B., J. Pendry, and D. Tsai, "Directed subwavelength imaging using a layered metal-dielectric system," *Physical Review B*, Vol. 74, No. 11, 115116, 2006.
15. Fang, N., H. Lee, C. Sun, and X. Zhang, "Sub-diffraction-limited optical imaging with a silver superlens," *Science*, Vol. 308, No. 5721, 534–537, 2005.
16. Lu, Z., C. Chen, C. A. Schuetz, S. Shi, J. A. Murakowski, G. J. Schneider, and D. W. Prather, "Subwavelength imaging by a flat cylindrical lens using optimized negative refraction," *Applied Physics Letters*, Vol. 87, No. 9, 091907–091907-3, 2005.
17. Paquay, M., J.-C. Iriarte, I. Ederra, R. Gonzalo, and P. de Maagt, "Thin AMC structure for radar cross-section reduction," *IEEE Transactions on Antennas and Propagation*, Vol. 55, No. 12, 3630–3638, 2007.
18. Iriarte, J.-C., M. Paquay, I. Ederra, R. Gonzalo, and P. de Maagt, "Combination of AMC and PEC cells for RCS applications," *2007 IEEE Antennas and Propagation Society International Symposium*, 865–868, 2007.
19. De Cos, M. E., Y. Alvarez-Lopez, and F. Las Heras Andres, "A novel approach for RCS reduction using a combination of artificial magnetic conductors," *Progress In Electromagnetics Research*, Vol. 107, 147–159, 2010.
20. Oraizi, H. and A. Abdolali, "Combination of MLS, GA & CG for the reduction of RCS of multilayered cylindrical structures composed of dispersive metamaterials," *Progress In Electromagnetics Research B*, Vol. 3, 227–253, 2008.
21. Pouliguen, P., R. Hémon, C. Bourlier, J.-F. Damiens, and J. Saillard, "Analytical formulae for radar cross section of flat plates in near field and normal incidence," *Progress In Electromagnetics Research B*, Vol. 9, 263–279, 2008.
22. Alexopoulos, A., "Effect of atmospheric propagation in RCS predictions," *Progress In Electromagnetics Research*, Vol. 101, 277–290, 2010.
23. N.-J. Li, C.-F. Hu, L.-X. Zhang, and J.-D. Xu, "Overview of RCS extrapolation techniques to aircraft targets," *Progress In Electromagnetics Research B*, Vol. 9, 249–262, 2008.
24. Lee, K.-C., C.-W. Huang, and M.-C. Fang, "Radar target recognition by projected features of frequency-diversity RCS," *Progress In Electromagnetics Research*, Vol. 81, 121–133, 2008.
25. Hady, L. K. and A. A. Kishk, "Electromagnetic scattering from conducting circular cylinder coated by meta-materials and loaded with helical strips under oblique incidence," *Progress In Electromagnetics Research B*, Vol. 3, 189–206, 2008.
26. Landy, N., S. Sajuyigbe, J. Mock, D. Smith, and W. Padilla, "Perfect metamaterial absorber," *Physical Review Letters*, Vol. 100, No. 20, 207402, 2008.
27. Wang, B., T. Koschny, and C. M. Soukoulis, "Wide-angle and polarization-independent chiral metamaterial absorber," *Physical Review B*, Vol. 80, No. 3, 33108, 2009.
28. Tao, H., N. I. Landy, C. M. Bingham, X. Zhang, R. D. Averitt, and W. J. Padilla, "A metamaterial absorber for the terahertz regime: Design, fabrication and characterization," arXiv preprint arXiv:0803.1646, Vol. 16, No. 10, 7181–7188, 2008.
29. Xu, H.-X., G.-M. Wang, M.-Q. Qi, J.-G. Liang, J.-Q. Gong, and Z.-M. Xu, "Triple-band polarization-insensitive wide-angle ultra-miniature metamaterial transmission line absorber," *Physical Review B*, Vol. 86, No. 20, 205104, 2012.
30. Watts, C., X. Liu, and W. Padilla, "Metamaterial electromagnetic wave absorbers," *Advanced Materials*, Vol. 24, No. 23, OP98–OP120, 2012.
31. Yang, X. M., X. Y. Zhou, Q. Cheng, H. F. Ma, and T. J. Cui, "Diffuse reflections by randomly gradient index metamaterials," *Optics Letters*, Vol. 35, No. 6, 808–810, 2010.
32. Zhang, Y., R. Mittra, B.-Z. Wang, and N.-T. Huang, "AMCs for ultra-thin and broadband RAM design," *Electronics Letters*, Vol. 45, No. 10, 484–485, 2009.
33. Iriarte, J. C., et al., "RCS reduction in a chessboard-like structure using AMC cells," *Proceedings EUCAP 2007*, 1–4, Nov. 11–16, 2007.
34. Li, H., B.-Z. Wang, and W. Shao, "Novel broadband reflectarray antenna with compound-cross-loop elements for millimeter-wave application," *Journal of Electromagnetic Waves and Applications*, Vol. 21, No. 10, 1333–1340, 2007.